Comput. Methods Appl. Mech. Engrg. 272 (2014) 1–16

Contents lists available at ScienceDirect

Comput. Methods Appl. Mech. Engrg.

journal homepage: www.elsevier.com/locate/cma

Recovery-based error estimator for stabilized finite element methods for the Stokes equation ☆

Lina Song [a,b], Yanren Hou [b,c,*], Zhiqiang Cai [d]

[a] College of Mathematics, Qingdao University, Qingdao 266071, China
[b] School of Mathematics and Statistics, Xi'an Jiaotong University, Xi'an 710049, China
[c] Center for Computational Geosciences, Xi'an Jiaotong University, Xi'an 710049, China
[d] Department of Mathematics, Purdue University, West Lafayette, IN 47907-2067, USA

ARTICLE INFO

Article history:
Received 31 May 2013
Received in revised form 30 December 2013
Accepted 6 January 2014
Available online 16 January 2014

Keywords:
Recovery-based error estimator
A posterior error estimates
Stabilized finite element method
Stokes equations
Adaptive method

ABSTRACT

A recovery-based error estimator is proposed and analyzed for stabilized P_1/P_0 (continuous linear velocity/constant pressure) finite element approximations to the Stokes equation. Reliability and efficiency of the estimator are established for various stabilized methods. For several test problems, numerical results show that our estimator is more accurate than the classical residual error estimator.

1. Introduction

Estimating and quantifying approximation errors are very important in both theory and practice of the finite element method. The a posteriori error estimation [1,23] may provide information of the magnitude and the distribution of the error, which, in turn, may be used for error control and local mesh refinement, respectively. The aim of this paper is to study a recovery-based a posteriori error estimator for various stabilized P_1/P_0 (continuous linear velocity/constant pressure) finite element approximations to the Stokes problem.

It is well known that the simplest finite element pair P_1/P_0 does not satisfy the inf-sup condition (see, e.g., [14]). To circumvent this difficulty, several types of stabilized finite element methods have been developed for the Stokes equation during the past several decades. Fundamentally, the quadratic form of the Stokes equation has no control on the pressure (see [2]). To gain the stability with respect to the pressure variable, one needs to add certain terms to the variational formulation. This is done through adding (I) a weighted least-squares term of the momentum equation (see, e.g., [3,5,13]); (II) the difference of the numerical pressure and its projection onto continuous piecewise linear finite element space (see [6,19,22,26]), the so-called projection stabilized method; and (III) the pressure jumps along interior sides (see [16,18]), the so-called penalizing jump stabilized method. The stabilized method in (I) is always consistent. When the pressure is continuous, the stabilized methods in (II) and (III) are also consistent. Moreover, the method in (II) is stabilization parameter free.

☆ Supported by NSF of China (Grant Nos. 11171269, 11201369 and 11201254) and PhD Programs Foundation of Ministry of Education of China (Grant No. 20110201110027).

* Corresponding author at: School of Mathematics and Statistics, Xi'an Jiaotong University, Xi'an 710049, China. Tel.: +86 2982663565.
E-mail address: yrhou@mail.xjtu.edu.cn (Y. Hou).

0045-7825/$ - see front matter © 2014 Elsevier B.V. All rights reserved.
http://dx.doi.org/10.1016/j.cma.2014.01.004

Residual-based a posteriori error estimators for the stabilized P_1/P_0 finite element methods have been studied by Kay and Silvester [17] and J. Wang, Y. Wang, and Ye [25] for the penalizing jump method and by Zheng, Hou and Shi [27] for the projection method.

In this paper, we study a recovery-based estimator for both the penalizing jump and the projection P_1/P_0 stabilized finite element methods. The recovery-based estimator was first introduced by Zienkiewicz and Zhu (see, e.g., [28,29]) and is defined as the L^2 norm of the difference between the numerical stress (or gradient) and the recovered stress (or gradient). Since the numerical stress is discontinuous, one recovers a stress in the continuous piecewise linear finite element space by averaging or the L^2 projection. An alternative recovery strategy, polynomial preserving recovery, was studied by Naga and Zhang [20]. For the Stokes equation, the recovery-based (ZZ) a posteriori error estimator for the nonconforming finite element approximation was studied by Carstensen and Funken [10].

The recovery-based (ZZ) error estimator was analyzed for the lowest order finite element approximation to the Poisson equation by Rodríguez [21] and Carstensen [11]. They provide some useful arguments to establish reliability and efficiency bounds. Our analysis may be regarded as a nontrivial extension of their arguments to the stabilized P_1/P_0 finite element approximation to the Stokes equation. For the continuous piecewise linear finite element approximation to the Poisson equation, the ZZ estimator is equivalent to the edge residual estimator, which is dominant in the residual-based estimator for the lowest order finite element method. However, such an equivalence is no longer valid for the stabilized P_1/P_0 approximation to the Stokes equation due to the discontinuous pressure. Alternatively, we make use of a property of the stabilized method to show the dominance of the recovery-based error estimator. This property of the stabilized method is the term reflecting that the inf-sup 'deficiency' of the unstable P_1/P_0 pair can be bounded by the true error. Finally, numerical results for several test problems are presented to show its practical effectivity.

The error estimator studied here possess the following features, and some of them are common for the recovery-based estimators. (1) Our numerical results show that the recovery-based estimator is more accurate than the residual estimator in [17,25]. (2) The estimator is reliable and efficient for both the stabilized methods. (3) Since the estimator uses no information of the underlying problem, it is easy to be applied to some other more complex models, such as Navier–Stokes problem, conduction convection problem, etc. (4) It is simple to be implemented.

The paper is organized as follows. In Section 2, we review the P_1/P_0 stabilized finite element methods for the Stokes equation. In Section 3, we propose the recovery-based error estimator and establish reliability and efficiency bounds. Numerical results are presented in Section 4, which confirm the theoretical results and provide a comparison of the estimator with the residual error estimator. A conclusion remark is presented in Section 5.

2. Stabilized P_1/P_0 approximations

We consider the Stokes problem with homogeneous Dirichlet boundary conditions in d-dimensional (d =2,3) bounded domain Ω. The problem reads: for given $\boldsymbol{f} \in L^2(\Omega)^d$, find the velocity $\boldsymbol{u}$ and the pressure p such that

$$\begin{cases} \operatorname{div} \boldsymbol{\sigma} + \boldsymbol{f} = 0 & \text{in } \Omega, \\ \boldsymbol{\sigma} := \nabla \boldsymbol{u} - p\, \boldsymbol{I} & \text{in } \Omega, \\ \operatorname{div} \boldsymbol{u} = 0 & \text{in } \Omega, \\ \boldsymbol{u} = 0 & \text{on } \partial\Omega. \end{cases} \tag{1}$$

Here $\boldsymbol{I}$ denotes the $d \times d$-identity matrix.

To establish the weak form of the above system, we introduce the following spaces

$$\boldsymbol{X}_0 := H_0^1(\Omega)^d \quad \text{and} \quad M := L_0^2(\Omega) = \left\{ q \in L^2(\Omega) : \int_\Omega q \mathrm{d}x = 0 \right\}.$$

Then the weak form of the Stokes problem (1) reads: find $(\boldsymbol{u}, p) \in \boldsymbol{X}_0 \times M$ such that

$$\mathcal{L}((\boldsymbol{u}, p), (\boldsymbol{v}, q)) = \boldsymbol{f}(\boldsymbol{v}) \quad \forall\ (\boldsymbol{v}, q) \in \boldsymbol{X}_0 \times M, \tag{2}$$

where the bilinear and linear forms are defined by

$$\mathcal{L}((\boldsymbol{u}, p), (\boldsymbol{v}, q)) = (\nabla \boldsymbol{u}, \nabla \boldsymbol{v}) - (p, \operatorname{div} \boldsymbol{v}) + (q, \operatorname{div} \boldsymbol{u}) \quad \text{and} \quad \boldsymbol{f}(\boldsymbol{v}) = (\boldsymbol{f}, \boldsymbol{v}).$$

Furthermore, the bilinear form $\mathcal{L}$ satisfies the inf-sup condition: there exists a positive constant β such that

$$\inf_{(\boldsymbol{u},p) \in \boldsymbol{X}_0 \times M} \sup_{(\boldsymbol{v},q) \in \boldsymbol{X}_0 \times M} \frac{\mathcal{L}((\boldsymbol{u}, p), (\boldsymbol{v}, q))}{|||(\boldsymbol{v}, q)||| \ |||(\boldsymbol{u}, p)|||} \geqslant \beta, \tag{3}$$

where the energy norm $|||\cdot|||$ is defined by $|||(\boldsymbol{v}, q)||| = (\|\boldsymbol{v}\|_1^2 + \|q\|^2)^{\frac{1}{2}}$. This ensures the unique solvability of (2); see [14].

Let $\tau_h = \{T\}$ be a finite element partition of the domain Ω with the mesh parameter $h = \max_{T \in \tau_h} \operatorname{diam}(T)$, where T can be triangle in 2-dimensions and tetrahedron in 3-dimensions. Assume that the triangulation τ_h is regular; i.e., the ratio h_T/ρ_T is bounded by

$$c_T := \sup\{h_T/\rho_T : T \in \tau_h, h > 0\} < \infty. \tag{4}$$

Here h_T denotes the diameter of the element T and ρ_T the diameter of the largest circle that may be inscribed in T. Denote by $\mathcal{S}_h$ the set of all sides in τ_h lying inside Ω. Each $e \in \mathcal{S}_h$ is an edge and a triangle in 2- and 3-dimensions, respectively. For any piecewise constant q and piecewise constant tensor $\boldsymbol{\tau}$, let

$$[q]_e := q|_{T_e^+} - q|_{T_e^-} \quad \text{and} \quad [\boldsymbol{\tau}]_e := \boldsymbol{\tau}|_{T_e^+} - \boldsymbol{\tau}|_{T_e^-}$$

denote their jumps on the side $e \in \mathcal{S}_h$, where T_e^+ and T_e^- are two elements sharing the common side e. Let us denote by h_e the size of a given side $e \in \mathcal{S}_h$. The norm

$$\|u\|_{\mathcal{S}_h} := \left(\sum_{e \in \mathcal{S}_h} h_e \|u\|_e^2 \right)^{\frac{1}{2}}$$

will prove useful in what follows.

Let us denote by

$$R_1(\Omega) = \{ v_h \in C^0(\Omega) : v_h|_T \in P_1(T) \quad \forall T \in \tau_h \},$$

where $P_1(T)$ is the space of linear polynomials on element T. Moreover, we introduce the piecewise constant finite element space

$$R_0(\Omega) = \{ q_h \in L^2(\Omega) : \ q_h|_T \in P_0(T) \quad \forall T \in \tau_h \},$$

where $P_0(T)$ is a constant polynomial space on element T.

In this paper, our main focus is the lowest-order conforming pair

$$\boldsymbol{X}_h = \boldsymbol{X}_0 \cap R_1(\Omega)^d \quad \text{and} \quad M_h = L_0^2(\Omega) \cap R_0(\Omega).$$

It is well known that finite element space pair $(\boldsymbol{X}_h, M_h)$ does not satisfy the discrete inf-sup condition. To use such simple P_1/P_0 finite element pair for numerically solving the Stokes Eqs. (1), some stabilized finite element methods are necessary. A kind of regularized stabilized discrete formulation is as follows: find $(\boldsymbol{u}_h, p_h) \in \boldsymbol{X}_h \times M_h$ satisfy

$$\mathcal{L}((\boldsymbol{u}_h, p_h), (\boldsymbol{v}_h, q_h)) + S(p_h, q_h) = \boldsymbol{f}(\boldsymbol{v}_h) \quad \forall \ (\boldsymbol{v}_h, q_h) \in \boldsymbol{X}_h \times M_h, \tag{5}$$

where $S(p_h, q_h) : \ M_h \times M_h \to \mathcal{R}$ is a symmetric stabilization term. Two specific choices of the stabilization term are defined below.

2.1. Penalizing jump stabilized method

The idea here is to stabilize the approximation by penalizing jumps in pressure across internal interelement sides; see [16,17]. The stabilization term is defined by

$$S(p_h, q_h) = \beta_0 \sum_{e \in \mathcal{S}_h} h_e \int_e [p_h]_e [q_h]_e \ \mathrm{ds} \quad \forall p_h, q_h \in M_h. \tag{6}$$

Here β_0 is a given stabilization parameter. It must be chosen carefully. For example, the numerical velocity field could no longer be regarded as be divergence free if β_0 is too large.

In addition, the stabilization term of consistently stabilized methods in [13,25] reads

$$S((\boldsymbol{u}_h, p_h), (\boldsymbol{v}_h, q_h)) = \gamma \sum_{T \in \tau_h} h_T^2 (\boldsymbol{f} + \Delta \boldsymbol{u}_h - \nabla p_h, -\tau \Delta \boldsymbol{v}_h + \nabla q_h) + \beta_0 \sum_{e \in \mathcal{S}_h} h_e \int_e [p_h]_e [q_h]_e \mathrm{ds} \quad \forall (\boldsymbol{v}_h, q_h) \in \boldsymbol{X}_h \times M_h. \tag{7}$$

For P_1/P_0 elements, the consistently stabilized method reduces to the penalizing jump stabilized method. The reason is the term $-\tau \Delta \boldsymbol{v}_h + \nabla q_h$ in (7) equals zero.

2.2. Projection stabilized method

The method uses the term that characterizes the inf-sup 'deficiency' of the unstable spaces to stabilize the approximation; see [6].

The stabilization term in (5) is given by

$$S(p_h, q_h) = (p_h - \Pi_1 p_h, q_h - \Pi_1 q_h) \quad \forall p_h, q_h \in M_h. \tag{8}$$

The operator Π_1 is defined by $\Pi_1 : L^2(\Omega) \mapsto R_1(\Omega)$.

In contrast to the penalizing jump stabilized methods, the projection method is parameter free, does not require side-based data structures, and always leads to symmetric linear systems.

Remark. The lowest-order conforming pair $(\boldsymbol{X}_h, M_h)$ satisfies a weak inf-sup condition

$$\sup_{\boldsymbol{v}_h\in\boldsymbol{X}_h}\frac{\int_\Omega q_h\nabla\cdot\boldsymbol{v}_h\mathrm{d}x}{\|\boldsymbol{v}_h\|_1}\geqslant c_1\|q_h\|-c_2\left(\sum_{e\in\mathcal{S}_h}h_e\|[q_h]_e\|_e^2\right)^{\frac{1}{2}}\quad\forall\ q_h\in M_h,$$

where c_1 and c_2 are positive constants independent of the mesh size; see [6].

The term $\left(\sum_{e\in\mathcal{S}_h}h_e\|[q_h]_e\|_e^2\right)^{\frac{1}{2}}$ quantifies the inf-sup 'deficiency' of the unstable pair. In some sense, the stabilized methods for P_1/P_0 approximation are designed to counterbalance this term. For instances, the stabilized formulation (5) can be rewritten as

$$\begin{aligned}&(\nabla\boldsymbol{u}_h,\nabla\boldsymbol{v}_h)-(\nabla\cdot\boldsymbol{v}_h,p_h)=(\boldsymbol{f},\boldsymbol{v}_h)\quad\forall\boldsymbol{v}_h\in\boldsymbol{X}_h,\\&(\nabla\cdot\boldsymbol{u}_h,q_h)+S(p_h,q_h)=0\quad\forall q_h\in M_h.\end{aligned}\tag{9}$$

The stabilization term $S(p_h,q_h)$ is added to the continuity equation to help offset the 'deficiency' term. Therefore, no matter the choice of stabilized method, the stabilization term is closely associated with $\left(\sum_{e\in\mathcal{S}_h}h_e\|[q_h]_e\|_e^2\right)^{\frac{1}{2}}$. Such connection will prove useful in showing that the recovery-based error estimator is reliable and efficient for various stabilized methods.

3. Recovery-based error estimator

To formulate the error estimator, we need some notations. We denote by $\mathcal{N}$ and $\mathcal{N}_h$ the vertices in τ_h and the vertices in τ_h lying inside Ω, respectively. For given $z\in\mathcal{N}$, we denote by ϕ_z the nodal basis function associated with z and set $\omega_z:=\mathrm{supp}\phi_z$, the union of all elements that share the same vertex z. $|T|$ denotes the volume of the element $T\in\tau_h$.

Let $(\boldsymbol{u}_h,p_h)$ be the numerical solution of the stabilized method (5) with stabilization term (6) or (8). We consider the stress tensor $\boldsymbol{\sigma}$ and its finite element approximation $\boldsymbol{\sigma}_h:=\nabla\boldsymbol{u}_h-p_h\boldsymbol{I}$. A recovery technique aims to construct $G(\boldsymbol{\sigma}_h)$ based on $\boldsymbol{\sigma}_h$ such that $G(\boldsymbol{\sigma}_h)$ approximates $\boldsymbol{\sigma}$ better than $\boldsymbol{\sigma}_h$ in some norm. In other words, $G(\boldsymbol{\sigma}_h)$ satisfies

$$\|\boldsymbol{\sigma}-G(\boldsymbol{\sigma}_h)\|\ll\|\boldsymbol{\sigma}-\boldsymbol{\sigma}_h\|.\tag{10}$$

The recovery technique is not only a postprocessing tool to improve the approximation, but also a way to construct a posteriori error estimator. Using the triangular inequality gives

$$1-\frac{\|\boldsymbol{\sigma}-G(\boldsymbol{\sigma}_h)\|}{\|\boldsymbol{\sigma}-\boldsymbol{\sigma}_h\|}\leqslant\frac{\|\boldsymbol{\sigma}_h-G(\boldsymbol{\sigma}_h)\|}{\|\boldsymbol{\sigma}-\boldsymbol{\sigma}_h\|}\leqslant1+\frac{\|\boldsymbol{\sigma}-G(\boldsymbol{\sigma}_h)\|}{\|\boldsymbol{\sigma}-\boldsymbol{\sigma}_h\|}.$$

Based on (10), $\|\boldsymbol{\sigma}-G(\boldsymbol{\sigma}_h)\|/\|\boldsymbol{\sigma}-\boldsymbol{\sigma}_h\|$ is much smaller than 1, therefore,

$$\frac{\|\boldsymbol{\sigma}_h-G(\boldsymbol{\sigma}_h)\|}{\|\boldsymbol{\sigma}-\boldsymbol{\sigma}_h\|}\approx1.$$

Namely $\|\boldsymbol{\sigma}_h-G(\boldsymbol{\sigma}_h)\|$ can be an error estimator to estimate the unknown true error $\|\boldsymbol{\sigma}-\boldsymbol{\sigma}_h\|$. Using the superconvergence patch recovery technique in [28], we recover the piecewise constant tensor $\boldsymbol{\sigma}_h$ to the continuous field, that is, the recovered stress tensor $G(\boldsymbol{\sigma}_h)\in R_1(\Omega)^{d\times d}$. In the following, we will show the construction of $G(\boldsymbol{\sigma}_h)$ in detail.

For any given tensor $\boldsymbol{\tau}\in R_0(\Omega)^{d\times d}$, we use the least square method to construct its continuous approximation. Let $\boldsymbol{\tau}_z$ be the constant valued tensor defined on ω_z, which minimizes the functional

$$J_z(\boldsymbol{\tau}_z)=\frac{1}{2}\int_{\omega_z}(\boldsymbol{\tau}-\boldsymbol{\tau}_z)^2\mathrm{d}x.\tag{11}$$

Then, these constant valued tensors $\{\boldsymbol{\tau}_z\}$ are interpolated to obtain the continuous approximation $G(\boldsymbol{\tau})$ over the whole domain,

$$G(\boldsymbol{\tau})=\sum_{z\in\mathcal{N}}\boldsymbol{\tau}_z\phi_z\quad\forall\boldsymbol{\tau}\in R_0(\Omega)^{d\times d}.$$

When choosing $\boldsymbol{\tau}=\boldsymbol{\sigma}_h$, the functional (11) can be simplified as

$$J_z(\boldsymbol{\tau}_z)=\frac{1}{2}\sum_{T\in\omega_z}|T|(\boldsymbol{\sigma}_T-\boldsymbol{\tau}_z)^2,$$

where $\boldsymbol{\sigma}_T$ is the restriction of $\boldsymbol{\sigma}_h$ on element T. It is easy to show that the minimal value point of the functional above is $\tilde{\boldsymbol{\tau}}_z=\sum_{T\in\omega_z}\frac{|T|}{|\omega_z|}\boldsymbol{\sigma}_T$. Therefore,

$$G(\boldsymbol{\sigma}_h)=\sum_{z\in\mathcal{N}}\tilde{\boldsymbol{\tau}}_z\phi_z.\tag{12}$$

Noticing the fact that the nodal value of $G(\boldsymbol{\sigma}_h)$ at z is area-weighted average of $\boldsymbol{\sigma}_h$ over ω_z, we actually have

$$G(\boldsymbol{\sigma}_h)(z)=\fint_{\omega_z}\boldsymbol{\sigma}_h\mathrm{d}x:=\int_{\omega_z}\boldsymbol{\sigma}_h\mathrm{d}x/\int_{\omega_z}1\mathrm{d}x.$$

Now we are in the position to give the recovery-based error estimator. Let

$$\eta_T := \|\boldsymbol{\sigma}_h - G(\boldsymbol{\sigma}_h)\|_T$$

be the local estimator and

$$\eta_R := \left(\sum_{T\in\tau_h}\eta_T^2\right)^{\frac{1}{2}}$$

be the global one.

To illustrate the property of the recovery-based error estimator, we introduce two inequalities.

One is the trace inequality. There exists $c > 0$, independent of the mesh size, such that

$$\|q_h\|_{\partial T} \leqslant c\ h_T^{-\frac{1}{2}}\|q_h\|_T \quad \forall q_h \in P_1(T). \tag{13}$$

Another is inverse inequality proposed in [11] for the efficiency of averaging estimators,

$$\|q_h - \fint_{\omega_z} q_h \mathrm{d}x\|_{\omega_z}^2 \leqslant c\sum_{e\in\mathcal{S}_z} h_e\|[q_h]_e\|_e^2 \quad \forall q_h \in R_0(\Omega), \tag{14}$$

where z is an arbitrary node, $\fint_{\omega_z} q_h \mathrm{d}x$ denotes the average of q_h over ω_z and $\mathcal{S}_z$ denotes the set of all sides sharing vertex z. For simplicity, symbol c (with or without a subscript) here and in the rest may represent different quantities at different occurrences, but it is always independent of the mesh size.

The recovery-based error estimator η_R has the following property.

Lemma 3.1. *Let $\boldsymbol{\sigma}_h$ be the finite element approximate stress tensor of problem (5). There exist two positive constants c_1 and c_2 independent of the mesh size such that*

$$c_1\ \|[\boldsymbol{\sigma}_h]_e\|_{\mathcal{S}_h} \leqslant \|\boldsymbol{\sigma}_h - G(\boldsymbol{\sigma}_h)\| \leqslant c_2\ \|[\boldsymbol{\sigma}_h]_e\|_{\mathcal{S}_h}.$$

Proof. For the first inequality, using the fact $[G(\boldsymbol{\sigma}_h)]_e = 0$ and the trace inequality (13) leads to

$$\|[\boldsymbol{\sigma}_h]_e\|_{\mathcal{S}_h} = \|[\boldsymbol{\sigma}_h - G(\boldsymbol{\sigma}_h)]_e\|_{\mathcal{S}_h} \leqslant c\ \|\boldsymbol{\sigma}_h - G(\boldsymbol{\sigma}_h)\|.$$

For the second inequality, by using the definition of $G(\boldsymbol{\sigma}_h)$ in (12), the Cauchy–Schwarz inequality and the inverse inequality (14), we obtain

$$\begin{aligned}\|\boldsymbol{\sigma}_h - G(\boldsymbol{\sigma}_h)\|^2 &= \left\|\sum_{i\in\mathcal{N}}(\boldsymbol{\sigma}_h - G(\boldsymbol{\sigma}_h)(i))\phi_i\right\|^2 = \int_\Omega\left|\sum_{i\in\mathcal{N}}(\boldsymbol{\sigma}_h - G(\boldsymbol{\sigma}_h)(i))\phi_i\right|^2\mathrm{d}x \leqslant \int_\Omega\left(\sum_{i\in\mathcal{N}}\phi_i\right)\left(\sum_{i\in\mathcal{N}}|\boldsymbol{\sigma}_h - G(\boldsymbol{\sigma}_h)(i)|^2\phi_i\right)\mathrm{d}x\\ &\leqslant \sum_{i\in\mathcal{N}}\int_{\omega_i}|\boldsymbol{\sigma}_h - G(\boldsymbol{\sigma}_h)(i)|^2\mathrm{d}x = \sum_{i\in\mathcal{N}}\|\boldsymbol{\sigma}_h - \fint_{\omega_i}\boldsymbol{\sigma}_h\mathrm{d}x\|_{\omega_i}^2 \leqslant c\ \|[\boldsymbol{\sigma}_h]_e\|_{\mathcal{S}_h}^2,\end{aligned}$$

where $|\cdot|$ stands for the Frobenius norm of tensor, namely, $|\boldsymbol{\tau}|^2 := \sum_{i=1}^2\sum_{j=1}^2\tau_{ij}^2$ for any tensor $\boldsymbol{\tau} = (\tau_{ij})$.

Combination of the above two inequalities ends the proof. □

Since the definition of operator Π_1 in stabilized method (8) in [6] is in the same fashion of the recovery operator $G(\cdot)$, we also have

$$c_1\ \|[q_h]_e\|_{\mathcal{S}_h} \leqslant \|q_h - \Pi_1 q_h\| \leqslant c_2\ \|[q_h]_e\|_{\mathcal{S}_h} \quad \forall q_h \in R_0(\Omega), \tag{15}$$

$$\|q_h - \Pi_1 q_h\| \leqslant c\ \|q_h\| \quad \forall q_h \in R_0(\Omega). \tag{16}$$

Thanks to the property of $G(\cdot)$ in (10), we have

$$\|\Pi_1 p_h - p_h\| \leqslant c\ \|p - p_h\|, \tag{17}$$

where p is the true pressure solution of (1) and p_h is the finite element approximation solution of (5).

Based on Lemma 3.1, we will show the reliability and efficiency of the recovery-based error estimator in following subsections.

Before moving onto next subsection, we illustrate the connection between $\|[\boldsymbol{\sigma}_h]_e\|_e$ and $\|[\boldsymbol{\sigma}_h\cdot\boldsymbol{n}_e]\|_e$, where $\boldsymbol{n}_e$ is the unit normal vector along $e \in \mathcal{S}_h$. This plays an important role in a posteriori error estimates for such a recovery-based error estimator. In 2-dimensions, we denote by $\boldsymbol{\tau}_e$ the unit tangential vector along e. Let

$$[\boldsymbol{\sigma}\cdot\boldsymbol{n}_e] := \boldsymbol{\sigma}|_{T_e^+}\cdot\boldsymbol{n}_e - \boldsymbol{\sigma}|_{T_e^-}\cdot\boldsymbol{n}_e$$
$$[\boldsymbol{\sigma}\cdot\boldsymbol{\tau}_e] := \boldsymbol{\sigma}|_{T_e^+}\cdot\boldsymbol{\tau}_e - \boldsymbol{\sigma}|_{T_e^-}\cdot\boldsymbol{\tau}_e$$

denote the jumps of the normal and tangential component of $\boldsymbol{\sigma}$ on the side e, respectively. Since $[\nabla \boldsymbol{u}_h \cdot \boldsymbol{\tau}_e] = 0$, we have

$$[\boldsymbol{\sigma}_h]_e = ([\boldsymbol{\sigma}_h \cdot \boldsymbol{n}_e],\ [\nabla \boldsymbol{u}_h \cdot \boldsymbol{\tau}_e] + [-p_h \boldsymbol{I}\boldsymbol{\tau}_e]) = ([\boldsymbol{\sigma}_h \cdot \boldsymbol{n}_e],\ [-p_h \boldsymbol{I}\boldsymbol{\tau}_e]).$$

Therefore,

$$\|[\boldsymbol{\sigma}_h]_e\|_e^2 = \|[\boldsymbol{\sigma}_h \cdot \boldsymbol{n}_e]\|_e^2 + \|[p_h]_e\|_e^2. \tag{18}$$

For the 3-dimensional case, we can obtain the above relation using the same argument except for introducing an additional unit tangential vector.

The above relation (18), together with Lemma 3.1, admits

$$\|[\boldsymbol{\sigma}_h \cdot \boldsymbol{n}_e]\|_{\mathcal{S}_h} \leqslant \|[\boldsymbol{\sigma}_h]_e\|_{\mathcal{S}_h} \leqslant c\ \eta_R, \tag{19}$$

$$\|[p_h]_e\|_{\mathcal{S}_h} \leqslant \|[\boldsymbol{\sigma}_h]_e\|_{\mathcal{S}_h} \leqslant c\ \eta_R. \tag{20}$$

3.1. Reliability

Firstly, we introduce some properties of the weighted Clément-type interpolation operator I_h defined in [12] in the following lemma. Such properties are often used for establishing the reliability bound of a posteriori error estimator; see [7,12,4].

Lemma 3.2. *There is a constant c, which depends only on the shape parameter c_T in (4), such that*

$$(\boldsymbol{f}, \boldsymbol{v} - I_h \boldsymbol{v}) \leqslant c\ H_{\boldsymbol{f}} \|\boldsymbol{v}\|_1 \quad \forall \boldsymbol{v} \in \boldsymbol{X}_0,$$

and

$$\left(\sum_{e \in \mathcal{S}_h} h_e^{-1} \|\boldsymbol{v} - I_h \boldsymbol{v}_h\|_e^2\right)^{\frac{1}{2}} \leqslant c\ \|\boldsymbol{v}\|_1 \quad \forall \boldsymbol{v} \in \boldsymbol{X}_0,$$

where $H_{\boldsymbol{f}} := \left(\sum_{z \in \mathcal{N} \setminus \mathcal{N}_h} |\omega_z|\ \|\boldsymbol{f}\|_{\omega_z}^2 + \sum_{z \in \mathcal{N}_h} |\omega_z|\ \|\boldsymbol{f} - \fint_{\omega_z} \boldsymbol{f}\, dx\|_{\omega_z}^2\right)^{\frac{1}{2}}$.

Proof. Refer to the Lemma 3.1, 6.1 and 6.2 in [12]. □

Remark. The second term in $H_{\boldsymbol{f}}$ is a higher-order term for $\boldsymbol{f} \in L^2(\Omega)^d$ and so is the first term for $\boldsymbol{f} \in L^p(\Omega)^d$ with $p > 2$; (see [12,7]).

Theorem 3.1. *(Reliability) Let $(\boldsymbol{u}, p)$ be the solution of problem (2) and $(\boldsymbol{u}_h, p_h)$ be finite element approximation solution of problem (5) with stabilization term (6) or (8). There exists a positive constant c independent of the mesh size such that*

$$|||(\boldsymbol{u} - \boldsymbol{u}_h, p - p_h)||| \leqslant c(\eta_R + H_{\boldsymbol{f}}).$$

Proof. Subtracting (5) from (2) gives

$$\mathcal{L}((\boldsymbol{u} - \boldsymbol{u}_h, p - p_h), (\boldsymbol{v}_h, q_h)) - S(p_h, q_h) = 0 \quad \forall (\boldsymbol{v}_h, q_h)\ \in \boldsymbol{X}_h \times M_h.$$

Taking $q_h = 0$ and $\boldsymbol{v}_h = I_h \boldsymbol{v}$ yields

$$\mathcal{L}((\boldsymbol{u} - \boldsymbol{u}_h, p - p_h), (I_h \boldsymbol{v}, 0)) = 0 \quad \forall\ \boldsymbol{v} \in \boldsymbol{X}_0. \tag{21}$$

For any $(\boldsymbol{v}, q) \in \boldsymbol{X}_0 \times M$, using integration by parts, the fact $\nabla \cdot \boldsymbol{\sigma}_h|_T = 0$ and (21) gives

$$\begin{aligned}
\mathcal{L}((\boldsymbol{u} - \boldsymbol{u}_h, p - p_h), (\boldsymbol{v}, q)) &= \mathcal{L}((\boldsymbol{u} - \boldsymbol{u}_h, p - p_h), (\boldsymbol{v} - I_h \boldsymbol{v}, q)) \\
&= (\nabla\ (\boldsymbol{u} - \boldsymbol{u}_h), \nabla(\boldsymbol{v} - I_h \boldsymbol{v})) - (p - p_h, \nabla \cdot (\boldsymbol{v} - I_h \boldsymbol{v})) + (q, \nabla \cdot (\boldsymbol{u} - \boldsymbol{u}_h)) \\
&= (\boldsymbol{\sigma}, \nabla(\boldsymbol{v} - I_h \boldsymbol{v})) + \sum_{T \in \tau_h} (\nabla \cdot \boldsymbol{\sigma}_h, \boldsymbol{v} - I_h \boldsymbol{v})_T + \sum_{e \in \mathcal{S}_h} ([\boldsymbol{\sigma}_h \cdot \boldsymbol{n}_e], \boldsymbol{v} - I_h \boldsymbol{v})_e - (q, \nabla \cdot \boldsymbol{u}_h) \\
&= (\boldsymbol{f}, \boldsymbol{v} - I_h \boldsymbol{v}) + \sum_{e \in \mathcal{S}_h} ([\boldsymbol{\sigma}_h \cdot \boldsymbol{n}_e], \boldsymbol{v} - I_h \boldsymbol{v})_e - (q, \nabla \cdot \boldsymbol{u}_h).
\end{aligned}$$

For the first two terms on the right hand side of the last expression, by using the Cauchy–Schwarz inequality, the properties of Clément interpolation in Lemma 3.2 and (19), we have

$$(\boldsymbol{f}, \boldsymbol{v} - I_h\boldsymbol{v}) + \sum_{e\in\mathcal{S}_h}([\boldsymbol{\sigma}_h\cdot\boldsymbol{n}_e], \boldsymbol{v} - I_h\boldsymbol{v})_e \leqslant H_{\boldsymbol{f}}\|\boldsymbol{v}\|_1 + \|[\boldsymbol{\sigma}_h\cdot\boldsymbol{n}_e]\|_{\mathcal{S}_h}\left(\sum_{e\in\mathcal{S}_h} h_e^{-1}\|\boldsymbol{v} - I_h\boldsymbol{v}\|_e^2\right)^{\frac{1}{2}} \leqslant c\left(H_{\boldsymbol{f}} + \|[\boldsymbol{\sigma}_h\cdot\boldsymbol{n}_e]\|_{\mathcal{S}_h}\right)\ \|\boldsymbol{v}\|_1$$
$$\leqslant c(H_{\boldsymbol{f}} + \eta_R)\ \|\boldsymbol{v}\|_1.$$

To estimate the term $(q, \nabla\cdot\boldsymbol{u}_h)$, we will use the second equation of (9),

$$(\nabla\cdot\boldsymbol{u}_h, q_h) + S(p_h, q_h) = 0 \quad \forall q_h \in M_h.$$

If the stabilization term is defined by (6), using the Cauchy–Schwarz inequality, the inverse inequality in (13) and (20) gives

$$\|\nabla\cdot\boldsymbol{u}_h\|^2 = -S(p_h, \nabla\cdot\boldsymbol{u}_h) = \beta_0\sum_{e\in\mathcal{S}_h} h_e\int_e [p_h]_e[\nabla\cdot\boldsymbol{u}_h]_e ds \leqslant c\ \|[p_h]_e\|_{\mathcal{S}_h}\ \|[\nabla\cdot\boldsymbol{u}_h]_e\|_{\mathcal{S}_h} \leqslant c\ \eta_R\ \|\nabla\cdot\boldsymbol{u}_h\|.$$

If the stabilization term is defined by (8), using the Cauchy–Schwarz inequality, the property of Π_1 in (15) and (16) and (20) gives

$$\|\nabla\cdot\boldsymbol{u}_h\|^2 = -S(p_h, \nabla\cdot\boldsymbol{u}_h) = -(p_h - \Pi_1 p_h, \nabla\cdot\boldsymbol{u}_h - \Pi_1(\nabla\cdot\boldsymbol{u}_h)) \leqslant \|p_h - \Pi_1 p_h\|\|\nabla\cdot\boldsymbol{u}_h - \Pi_1(\nabla\cdot\boldsymbol{u}_h)\|$$
$$\leqslant c\ \|[p_h]_e\|_{\mathcal{S}_h}\ \|\nabla\cdot\boldsymbol{u}_h\| \leqslant c\ \eta_R\ \|\nabla\cdot\boldsymbol{u}_h\|.$$

Therefore, we get

$$(\nabla\cdot\boldsymbol{u}_h, q) \leqslant \|\nabla\cdot\boldsymbol{u}_h\|\ \|q\| \leqslant c\ \eta_R\ \|q\|.$$

The combination of above inequalities yields

$$\mathcal{L}((\boldsymbol{u} - \boldsymbol{u}_h, p - p_h), (\boldsymbol{v}, q)) \leqslant c\ (H_{\boldsymbol{f}} + \eta_R)\ (\|\boldsymbol{v}\|_1 + \|q\|).$$

By the inf-sup condition (3), we have

$$|||(\boldsymbol{u} - \boldsymbol{u}_h, p - p_h)||| \leqslant \beta^{-1}\sup_{(\boldsymbol{v},q)\in\boldsymbol{X}_0\times M}\frac{\mathcal{L}((\boldsymbol{u} - \boldsymbol{u}_h, p - p_h), (\boldsymbol{v}, q))}{|||(\boldsymbol{v}, q)|||} \leqslant c\ (\eta_R + H_{\boldsymbol{f}}).$$

It completes the proof of the reliability. □

3.2. Efficiency

Using Lemma 3.1 and (18), we have

$$\eta_R \leqslant c\ \|[\boldsymbol{\sigma}_h]_e\|_{\mathcal{S}_h} = c\ (\|[\boldsymbol{\sigma}_h\cdot\boldsymbol{n}_e]\|_{\mathcal{S}_h} + \|[p_h]_e\|_{\mathcal{S}_h}). \tag{22}$$

To prove the efficiency of the recovery-based error estimator η_R, we firstly estimate

$$\|[\boldsymbol{\sigma}_h\cdot\boldsymbol{n}_e]\|_{\mathcal{S}_h} \quad \text{and} \quad \|[p_h]_e\|_{\mathcal{S}_h},$$

separately, and have following lemmas.

Lemma 3.3. *Let $\boldsymbol{\sigma}$ be the stress tensor of problem (2) and $\boldsymbol{\sigma}_h$ be the finite element approximate stress tensor of problem (5) with stabilization term (6) or (8). There exists a positive constant c independent of the mesh size such that*

$$h_e^{\frac{1}{2}}\|[\boldsymbol{\sigma}_h\cdot\boldsymbol{n}_e]\|_e \leqslant c\|\boldsymbol{\sigma} - \boldsymbol{\sigma}_h\|_{\omega_e} + ch_e\inf_{\boldsymbol{f}_h\in\boldsymbol{X}_h}\|\boldsymbol{f} - \boldsymbol{f}_h\|_{\omega_e},$$

where ω_e denotes the union of the two elements sharing the same side e.

Proof. For any interior side e, we introduce the bubble function $\psi_e = 4\ \Pi_{z\in\mathcal{N}_e}\phi_z$, where $\mathcal{N}_e$ denotes the vertices of the side e.
For any polynomial tensor $\boldsymbol{\sigma}$, we have the following estimates (see 2.11 in [4]),

$$\|\boldsymbol{\sigma}\|_e \leqslant \gamma_1\|\psi_e^{\frac{1}{2}}\boldsymbol{\sigma}\|_e, \tag{23}$$
$$\|\nabla(\psi_e\boldsymbol{\sigma})\|_T \leqslant \gamma_2 h_e^{-\frac{1}{2}}\|\boldsymbol{\sigma}\|_e, \tag{24}$$
$$\|\psi_e\boldsymbol{\sigma}\|_T \leqslant \gamma_3 h_e^{\frac{1}{2}}\|\boldsymbol{\sigma}\|_e. \tag{25}$$

If we denote $W_e = \psi_e[\boldsymbol{\sigma}_h\cdot\boldsymbol{n}_e]$, by using (24) and (25) we obtain

$$\|\nabla W_e\|_T \leqslant \gamma_2 h_e^{-\frac{1}{2}}\|[\boldsymbol{\sigma}_h\cdot\boldsymbol{n}_e]\|_e, \tag{26}$$
$$\|W_e\|_T \leqslant \gamma_3 h_e^{\frac{1}{2}}\|[\boldsymbol{\sigma}_h\cdot\boldsymbol{n}_e]\|_e. \tag{27}$$

Then by using (23), (26), (27), integration by parts and the Cauchy–Schwarz inequality, we get

$$\gamma_1^{-2}\|[\boldsymbol{\sigma}_h\cdot\boldsymbol{n}_e]\|_e^2 \leqslant \int_e [\boldsymbol{\sigma}_h\cdot\boldsymbol{n}_e]W_e \mathrm{d}x = \sum_{i=1}^{2}\int_{T_i} \operatorname{div}\,\boldsymbol{\sigma}_h W_e + \boldsymbol{\sigma}_h\nabla W_e \mathrm{d}x = \sum_{i=1}^{2}\int_{T_i} \boldsymbol{f}W_e - (\boldsymbol{\sigma}-\boldsymbol{\sigma}_h)\nabla W_e \mathrm{d}x$$
$$\leqslant \sum_{i=1}^{2}\Big(\|\boldsymbol{f}\|_{T_i}\|W_e\|_{T_i} + ||\boldsymbol{\sigma}-\boldsymbol{\sigma}_h||_{T_i}\|\nabla W_e\|_{T_i}\Big) \leqslant \sum_{i=1}^{2}\Big(\gamma_3 h_e^{\frac{1}{2}}\|\boldsymbol{f}\|_{T_i} + \gamma_2 h_e^{-\frac{1}{2}}||\boldsymbol{\sigma}-\boldsymbol{\sigma}_h||_{T_i}\Big)\|[\boldsymbol{\sigma}_h\cdot\boldsymbol{n}_e]\|_e.$$

Consider an arbitrary function $\boldsymbol{f}_h \in \boldsymbol{X}_h$, since $\nabla\cdot\boldsymbol{\sigma}_h|_T = 0$, we obtain

$$h_e^{\frac{1}{2}}\|[\boldsymbol{\sigma}_h\cdot\boldsymbol{n}_e]\|_e \leqslant c||\boldsymbol{\sigma}-\boldsymbol{\sigma}_h||_{\omega_e} + ch_e(\|\boldsymbol{f}-\boldsymbol{f}_h\|_{\omega_e} + \|\boldsymbol{f}_h+\nabla\cdot\boldsymbol{\sigma}_h\|_{\omega_e}). \tag{28}$$

Next, we estimate the term $\|\boldsymbol{f}_h+\nabla\cdot\boldsymbol{\sigma}_h\|_{\omega_e}$.

For any element T, we use the bubble function $\psi_T = 27\ \Pi_{z\in\mathcal{N}_T}\phi_z$.For any polynomial v, we have the following estimates hold (see 2.11 in [4]),

$$\|v\|_T \leqslant \gamma_4\|\psi_T^{\frac{1}{2}}v\|_T, \tag{29}$$
$$\|\nabla(\psi_T v)\|_T \leqslant \gamma_5 h_T^{-1}\|v\|_T, \tag{30}$$

Define $W_T = \psi_T(\boldsymbol{f}_h+\nabla\cdot\boldsymbol{\sigma}_h)$. Using (30) and the property of bubble function yields

$$\|\nabla W_T\|_T \leqslant \gamma_5 h_T^{-1}\|\boldsymbol{f}_T+\nabla\cdot\boldsymbol{\sigma}_h\|_T, \tag{31}$$

$$\|W_T\|_T \leqslant \|\boldsymbol{f}_h+\nabla\cdot\boldsymbol{\sigma}_h\|_T. \tag{32}$$

Using (29), (31), (32), integration by parts and the Cauchy–Schwarz inequality gives

$$\gamma_4^{-2}\|\boldsymbol{f}_h+\nabla\cdot\boldsymbol{\sigma}_h\|_T^2 \leqslant \int_T \psi_T(\boldsymbol{f}_h+\nabla\cdot\boldsymbol{\sigma}_h)^2\mathrm{d}x = \int_T(\boldsymbol{f}+\nabla\cdot\boldsymbol{\sigma}_h)W_T\mathrm{d}x + \int_T(\boldsymbol{f}_h-\boldsymbol{f})W_T\mathrm{d}x$$
$$= \int_T(\boldsymbol{\sigma}-\boldsymbol{\sigma}_h)\nabla W_T\mathrm{d}x + \int_T(\boldsymbol{f}_h-\boldsymbol{f})W_T\mathrm{d}x \leqslant ||\boldsymbol{\sigma}-\boldsymbol{\sigma}_h||_T\|\nabla W_T\|_T + \|\boldsymbol{f}_h-\boldsymbol{f}\|_T\|W_T\|_T$$
$$\leqslant \Big(\gamma_2 h_T^{-1}||\boldsymbol{\sigma}-\boldsymbol{\sigma}_h||_T + \|\boldsymbol{f}_h-\boldsymbol{f}\|_T\Big)\|\boldsymbol{f}_h+\nabla\cdot\boldsymbol{\sigma}_h\|_T.$$

So, we obtain

$$\|\boldsymbol{f}_h+\nabla\cdot\boldsymbol{\sigma}_h\|_T \leqslant \gamma_1^2\gamma_2 h_T^{-1}||\boldsymbol{\sigma}-\boldsymbol{\sigma}_h||_T + \gamma_1^2\|\boldsymbol{f}_h-\boldsymbol{f}\|_T,$$

which together with (28) gives

$$h_e^{\frac{1}{2}}\|[\boldsymbol{\sigma}_h\cdot\boldsymbol{n}_e]\|_e \leqslant c\ ||\boldsymbol{\sigma}-\boldsymbol{\sigma}_h||_{\omega_e} + c\ h_e \inf_{\boldsymbol{f}_h\in\boldsymbol{X}_h}\|\boldsymbol{f}-\boldsymbol{f}_h\|_{\omega_e}.$$

This completes the proof. □

Lemma 3.4. *Let $(\boldsymbol{u},p)$ be the solution of problem (2) and $(\boldsymbol{u}_h,p_h)$ be the finite element approximation solution of problem (5) with stabilization term (6) or (8). There exists a positive constant c independent of the mesh size such that*

$$\|[p_h]_e\|_{\mathcal{S}_h}^2 \leqslant c\sum_{e\in\mathcal{S}_h} h_e^{-1}\|(\boldsymbol{u}-\boldsymbol{u}_h)\cdot\boldsymbol{n}_e\|_e^2.$$

Proof. Using the second equation of (9) and letting $q_h = p_h$ give

$$(\nabla\cdot\boldsymbol{u}_h, p_h) + S(p_h,p_h) = 0.$$

We use the fact that $\nabla\cdot\boldsymbol{u} = 0$ and $\nabla p_h|_T = 0$, the integration by parts and the Cauchy–Schwarz inequality to get

$$S(p_h,p_h) = -(\nabla\cdot\boldsymbol{u}_h,p_h) = (\nabla\cdot(\boldsymbol{u}-\boldsymbol{u}_h),p_h) = \sum_{e\in\mathcal{S}_h}((\boldsymbol{u}-\boldsymbol{u}_h)\cdot\boldsymbol{n}_e,[p_h]_e)_e - \sum_{T\in\tau_h}(\boldsymbol{u}-\boldsymbol{u}_h,\nabla p_h)_T$$
$$\leqslant \left(\sum_{e\in\mathcal{S}_h} h_e^{-1}\|(\boldsymbol{u}-\boldsymbol{u}_h)\cdot\boldsymbol{n}_e\|_e^2\right)^{\frac{1}{2}}\|[p_h]_e\|_{\mathcal{S}_h}. \tag{33}$$

On another hand, we estimate the stabilization term $S(p_h,p_h)$ in two cases.

If the stabilization term is defined by (6), then

$$S(p_h,p_h) \geqslant c\ \|[p_h]_e\|_{\mathcal{S}_h}^2.$$

If the stabilization term is defined by (8), then using the property of Π_1 in (15) gives

$$S(p_h, p_h) = \|p_h - \Pi_1 p_h\|^2 \geqslant c \, \|[p_h]_e\|^2_{\mathcal{S}_h}.$$

Combining above equations with (33) leads to

$$\|[p_h]_e\|_{\mathcal{S}_h} \leqslant c \left(\sum_{e \in \mathcal{S}_h} h_e^{-1} \|(\boldsymbol{u} - \boldsymbol{u}_h) \cdot \boldsymbol{n}_e\|_e^2 \right)^{\frac{1}{2}}.$$

This completes the proof. □

Next we use the trace inequality and the Aubin-Nitsche duality argument to estimate $\sum_{e \in \mathcal{S}_h} h_e^{-1} \|(\boldsymbol{u} - \boldsymbol{u}_h) \cdot \boldsymbol{n}_e\|_e^2$ appearing in Lemma 3.4.

Lemma 3.5. *Let $(\boldsymbol{u}, p)$ be the solution of problem (2) and $(\boldsymbol{u}_h, p_h)$ be the finite element approximate solution of problem (5) with stabilization term (6) or (8). There exists a positive constant c independent of the mesh size such that*

$$\sum_{e \in \mathcal{S}_h} h_e^{-1} \|(\boldsymbol{u} - \boldsymbol{u}_h) \cdot \boldsymbol{n}_e\|_e^2 \leqslant c \, |||(\boldsymbol{u} - \boldsymbol{u}_h, p - p_h)|||^2.$$

Proof. Using the trace inequality, we have

$$\sum_{e \in \mathcal{S}_h} h_e^{-1} \|(\boldsymbol{u} - \boldsymbol{u}_h) \cdot \boldsymbol{n}_e\|_e^2 \leqslant c \, h^{-1} \|\boldsymbol{u} - \boldsymbol{u}_h\| \|\boldsymbol{u} - \boldsymbol{u}_h\|_1. \tag{34}$$

To estimate $\|\boldsymbol{u} - \boldsymbol{u}_h\|$, we use the Aubin-Nitsche duality argument.

For $(\varphi, \phi) \in L^2(\Omega)^2 \times (H^1(\Omega) \cap L_0^2(\Omega))$, consider the dual Stokes problem: seek $(\Phi, \Psi) \in (H^2(\Omega)^2 \cap H_0^1(\Omega)^2) \times (H^1(\Omega) \cap L_0^2(\Omega))$ such that

$$\mathcal{L}((\boldsymbol{v}, q), (\Phi, \Psi)) = (\varphi, \boldsymbol{v}) + (\phi, q) \quad \forall \, (\boldsymbol{v}, q) \in \boldsymbol{X}_0 \times M. \tag{35}$$

This problem admits a unique solution (Φ, Ψ) satisfying

$$\|\Phi\|_2 + \|\Psi\|_1 \leqslant c \, (\|\varphi\| + \|\phi\|_1). \tag{36}$$

Moreover, there exist $\Phi_h \in \boldsymbol{X}_h$ and $\Psi_h \in M_h$ such that

$$\|\Phi - \Phi_h\|_1 \leqslant c \, h \, \|\Phi\|_2 \quad \text{and} \quad \|\Psi - \Psi_h\| \leqslant c \, h \, \|\Psi\|_1. \tag{37}$$

Taking $(\boldsymbol{v}, q) = (\boldsymbol{u} - \boldsymbol{u}_h, p - p_h)$ in (35) yields

$$\mathcal{L}((\boldsymbol{u} - \boldsymbol{u}_h, p - p_h), (\Phi, \Psi)) = (\varphi, \boldsymbol{u} - \boldsymbol{u}_h) + (\phi, p - p_h). \tag{38}$$

In addition, subtracting (5) from (2) gives

$$\mathcal{L}((\boldsymbol{u} - \boldsymbol{u}_h, p - p_h), (\boldsymbol{v}_h, q_h)) - S(p_h, q_h) = 0 \quad \forall (\boldsymbol{v}_h, q_h) \in \boldsymbol{X}_h \times M_h.$$

Taking $(\boldsymbol{v}_h, q_h) = (\Phi_h, \Psi_h)$ admits

$$\mathcal{L}((\boldsymbol{u} - \boldsymbol{u}_h, p - p_h), (\Phi_h, \Psi_h)) - S(p_h, \Psi_h) = 0,$$

which together with (38) leads to

$$(\varphi, \boldsymbol{u} - \boldsymbol{u}_h) + (\phi, p - p_h) = \mathcal{L}((\boldsymbol{u} - \boldsymbol{u}_h, p - p_h), (\Phi - \Phi_h, \Psi - \Psi_h)) + S(p_h, \Psi_h). \tag{39}$$

Now we estimate the term $S(p_h, \Psi_h)$ in two cases.

Case 1. If the stabilization term is defined by (6), then using the Cauchy–Schwarz inequality, the property of Π_1 in (15) and (16) and the trace inequality (13) gives

$$S(p_h, \Psi_h) = \beta_0 \sum_{e \in \mathcal{S}_h} h_e \int_e [p_h]_e [\Psi_h]_e \mathrm{d}s \leqslant c \, \|[p_h]_e\|_{\mathcal{S}_h} \, \|[\Psi_h]_e\|_{\mathcal{S}_h} \leqslant c \, \|(I - \Pi_1) p_h\| \, \|[\Psi_h - \Psi]_e\|_{\mathcal{S}_h} \leqslant c \, \|p - p_h\| \, \|\Psi_h - \Psi\|.$$

Case 2. If the stabilization term is defined by (8), then

$$S(p_h, \Psi_h) = ((I - \Pi_1) p_h, (I - \Pi_1) \Psi_h) \leqslant c \, \|(I - \Pi_1) p_h\| \, \|[\Psi_h - \Psi]_e\|_{\mathcal{S}_h} \leqslant c \, \|p - p_h\| \, \|\Psi_h - \Psi\|.$$

Combining above expressions with (39) and using the continuity of $\mathcal{L}(\cdot, \cdot)$, (36) and (37) give

$$(\varphi, \boldsymbol{u}-\boldsymbol{u}_h)+(\phi, p-p_h) \leqslant c\ |||(\boldsymbol{u}-\boldsymbol{u}_h),(p-p_h)|||\,|||(\Phi-\Phi_h),(\Psi-\Psi_h)||| + c\ \|p-p_h\|\,\|\Psi_h-\Psi\|$$
$$\leqslant c\ h\ (\|\boldsymbol{u}-\boldsymbol{u}_h\|_1+\|p-p_h\|)(\|\Phi\|_2+\|\Psi\|_1) \leqslant c\ h\ (\|\boldsymbol{u}-\boldsymbol{u}_h\|_1+\|p-p_h\|)(\|\varphi\|_0+\|\phi\|_1).$$

Therefore

$$\|\boldsymbol{u}-\boldsymbol{u}_h\|+\|p-p_h\|_{-1} \leqslant c\ h\ (\|\boldsymbol{u}-\boldsymbol{u}_h\|_1+\|p-p_h\|),$$

which together with (34) yields

$$\sum_{e\in\mathcal{S}_h} h_e^{-1}\|(\boldsymbol{u}-\boldsymbol{u}_h)\cdot\boldsymbol{n}_e\|_e^2 \leqslant c\ (\|\boldsymbol{u}-\boldsymbol{u}_h\|_1+\|p-p_h\|)\|\boldsymbol{u}-\boldsymbol{u}_h\|_1 \leqslant c\ |||(\boldsymbol{u}-\boldsymbol{u}_h),(p-p_h)|||^2.$$

This completes the proof. □

Now we are in the position to present the main results of this subsection.

Theorem 3.2. *(Efficiency) Let $(\boldsymbol{u},p)$ be the solution of problem (2) and $(\boldsymbol{u}_h,p_h)$ be the finite element approximate solution of problem (5) with stabilization term (6) or (8). There exists a positive constant c independent of the mesh size such that*

$$\eta_R \leqslant c\ |||(\boldsymbol{u}-\boldsymbol{u}_h,p-p_h)||| + c\sum_{e\in\mathcal{S}_h} h_e \inf_{\boldsymbol{f}_h\in\boldsymbol{X}_h}\|\boldsymbol{f}-\boldsymbol{f}_h\|_{\omega_e}.$$

Proof. Using (22), Lemma 3.3, Lemma 3.4 and Lemma 3.5 gives

$$\eta_R \leqslant c\ (\|[\boldsymbol{\sigma}_h\cdot\boldsymbol{n}_e]\|_{\mathcal{S}_h}+\|[p_h]_e\|_{\mathcal{S}_h}) \leqslant c\ \|\boldsymbol{\sigma}-\boldsymbol{\sigma}_h\| + c\sum_{e\in\mathcal{S}_h} h_e \inf_{\boldsymbol{f}_h\in\boldsymbol{X}_h}\|\boldsymbol{f}-\boldsymbol{f}_h\|_{\omega_e} + \left(\sum_{e\in\mathcal{S}_h} h_e^{-1}\|(\boldsymbol{u}-\boldsymbol{u}_h)\cdot\boldsymbol{n}_e\|_e^2\right)^{\frac{1}{2}}$$
$$\leqslant c\ |||(\boldsymbol{u}-\boldsymbol{u}_h),(p-p_h)||| + c\sum_{e\in\mathcal{S}_h} h_e \inf_{\boldsymbol{f}_h\in\boldsymbol{X}_h}\|\boldsymbol{f}-\boldsymbol{f}_h\|_{\omega_e}.$$

This completes the proof of the efficiency. □

4. Numerical results

In this section, we present a selection of numerical results for three purposes: (1) showing that the recovery-based error estimator works well for general P_1/P_0 stabilized methods, (2) presenting the practical effectivity of the recovery-based error estimator, and (3) showing the recovery-based estimator η_R is more exact than the residual error estimator η_E in [12,25], which is defined by $\eta_E := \left(\sum_{T\in\tau_h}\eta_{e,T}^2\right)^{\frac{1}{2}}$ with

$$\eta_{e,T}^2 := \|\nabla\cdot\boldsymbol{u}_h\|_T^2 + \frac{1}{2}\sum_{e\in\partial T\cap\Omega} h_e^{\frac{1}{2}}\|[\boldsymbol{\sigma}_h\cdot\boldsymbol{n}_e]\|_e^2.$$

We consider three 2-dimensional numerical tests. The first one is a flow problem with a smooth solution. The second one is a flow problem in a singular L-shape domain. The third one models a flow problem in a cracked domain with a singular solution. The experiments are implemented by the public software Freefem++ [15].

In order to illustrate the recovery-based error estimator η_R is independent of the choice of the specific stabilized method, we use the adaptive strategy based on η_R for two stabilized methods for the Stokes problem. One is the penalizing jump stabilized method, namely, the stabilized method (5) with stabilization term (6). We choose the stabilization parameter $\beta_0 = 0.05$. Another is the projection stabilized method, namely, the stabilized method (5) with stabilization term (8).

4.1. Mesh refinement strategy

The mesh refinement strategy we used in FreeFem++ [15] is as follows.

Step 1. Given a triangulation τ^j. Compute an n-dimensional vector $\boldsymbol{h}^j$. Here n denotes the number of the vertexes of τ^j and the ith ($1\leqslant i\leqslant n$) component of $\boldsymbol{h}^j$ is the average length of the sides sharing the ith vertex.
Step 2. For every element $T\in\tau^j$, compute a local error estimator η_T^j (i.e., either η_T or $\eta_{e,T}$) and denote $\bar{\eta}^j := \sum_{T\in\tau^j}\eta_T^j/\sum_{T\in\tau^j}1$, the mean value of η_T^j over τ^j.
Step 3. Give the new size $\boldsymbol{h}^{j+1}$ by the following formulae

$$\boldsymbol{h}^{j+1} = \frac{\boldsymbol{h}^j}{f(\eta_T^j)}$$

where f is a user function defined by

$$f = \min(\max(\eta_T^j / c\ \bar{\eta}^j, 1.0), 3.0),$$

and c is a user defined coefficient generally close to 1.

Step 4. Get the new mesh τ^{j+1} by using a variable metric/ Delaunay automatic meshing algorithm in Freefem++ with the mesh size field $\boldsymbol{h}^{j+1}$.

For simplicity, in all experiments, we choose $c = 0.8$. One possible adaptive strategy is as follows. Given a user-specified tolerance η^* and an initial mesh τ^0. Refine the mesh by using the above mesh refinement strategy until the global error estimator η (i.e., either η_R or η_E) satisfies $\eta \leqslant \eta^*$.

For the sake of convenience, we introduce the following notions.

- DOF^j:= number of elements for the triangulation τ^j;
- $\boldsymbol{e}_r^j$:=$|||(\boldsymbol{u} - \boldsymbol{u}_h^j, p - p_h^j)|||/|||(\boldsymbol{u}, p)|||$ denotes relative error in the energy norm.
- $\eta_{R,r}$:=$\eta_R/|||(\boldsymbol{u}, p)|||$ denotes the relative value of global recovery-based estimator.
- $\eta_{E,r}$:=$\eta_E/|||(\boldsymbol{u}, p)|||$ denotes the relative value of global residual estimator.
- Order:=$\frac{2\log(\boldsymbol{e}_r^{j+1}/\boldsymbol{e}_r^j)}{\log(\mathrm{DOF}^j/\mathrm{DOF}^{j+1})}$ denotes the convergence rate of the error.
- E_R:=$\eta_{R,r}/\boldsymbol{e}_r$ denotes effectivity index for the global recovery-based estimator η_R.
- E_E:=$\eta_{E,r}/\boldsymbol{e}_r$ denotes effectivity index for the global residual estimator η_E.

4.2. A smooth problem

The first example is a flow problem with a smooth solution, given by

$$u_1 = 2\pi \sin^2(\pi x)\sin(\pi y)\cos(\pi y),$$
$$u_2 = -2\pi \sin(\pi x)\cos(\pi x)\sin^2(\pi y),$$
$$p = \cos(\pi x)\cos(\pi y),$$

where domain $\Omega = (0,1) \times (0,1)$.

Firstly, we consider the penalizing jump stabilized method and report numerical results for adaptive refinements via this stabilized method with estimator η_R in Table 1. We can see the refinements get good approximate solution as $h \to 0$ and nearly optimal convergence order (about 1.0). In addition, the effectivity index E_R approaches to 1.0, which illustrates estimator η_R performs well for the penalizing jump stabilized method.

Secondly, we use the adaptive strategy for the projection stabilized method. The numerical results are presented in Table 2. They show the convergence rate of the error in energy norm keeps order 1.0, and the estimator η_R is almost exact. They are consistent with the results in Table 1.

From all the results in Table 1 and 2, we can see the recovery-based error estimator η_R works well for general P_1/P_0 stabilized methods.

Table 1
Results for adaptive refinements via penalizing jump stabilized method with η_R.

Level	DOF^j	$\boldsymbol{e}_r^j$	Order	$\eta_{R,r}$	E_R
0	208	0.3026	–	0.2989	0.9881
1	314	0.2332	1.2644	0.2323	0.9961
2	513	0.1732	1.2107	0.1759	1.0151
3	927	0.1304	0.9607	0.1301	0.9983
4	1597	0.0971	1.0858	0.0971	1.0011

Table 2
Results for adaptive refinements via projection stabilized method with η_R.

Level	DOF^j	$\boldsymbol{e}_r^j$	Order	$\eta_{R,r}$	E_R
0	208	0.3498	–	0.3362	0.9611
1	321	0.2526	1.4992	0.2513	0.9947
2	533	0.1885	1.1549	0.1882	0.9986
3	978	0.1363	1.0671	0.1353	0.9925
4	1708	0.1025	1.0221	0.1018	0.9926

4.3. L-shape domain problem

The second example is a flow problem in the L-shape domain $\Omega = (-1,1)^2 - [0,1]^2$. The right hand side $\boldsymbol{f}$ of the Stokes problem (1) is determined by exact velocity $\boldsymbol{u} = (u_1, u_2)$ and pressure p:

$$u_1(x,y) = \frac{y-0.1}{\sqrt{(x-0.1)^2+(y-0.1)^2}},$$
$$u_2(x,y) = -\frac{x-0.1}{\sqrt{(x-0.1)^2+(y-0.1)^2}},$$
$$p(x,y) = \frac{1}{y+1.05} - \frac{\log(2.05)+\log(1.05)-2\log(0.05)}{3}.$$

We note that both the velocity $\boldsymbol{u}$ and the pressure p are smooth in the domain. However, it is clear that $\boldsymbol{u}$ and p are singular at the point (0.1,0.1) and along the line $y = -1.05$, respectively.

Firstly, we consider the projection stabilized method. In order to show the practical effectivity of the recovery-based estimator η_R, we compare the results of adaptive refinements with those of uniform refinements, also compare the effectivity index of η_R with that of the residual estimator η_E.

Table 3–5 show the numerical results for uniform/adaptive refinements with recovery-based estimator η_R and residual estimator η_E. Fig. 1 shows the adaptive meshes based on the both error estimators. The observations and conclusions of this experiment are presented as follows.

- The stabilized method based on adaptive refinements obtains much better approximate solution than that based on uniform refinements. To get the similar accuracy, i.e. the relative error $\boldsymbol{e}_r = 0.13$, it uses 4258 elements in the uniform case (see Level 4 in Table 3), while it only uses 820 elements in the adaptive case with η_R (see Level 2 in Table 4 and 1130 elements with η_E (see Level 3 in Table 5). Moreover, the numerical results show that the convergence rate for adaptive refinements is a little bit higher than that for the uniform case (see Order in Table 3–5).
- Mesh refinements based on both estimator η_R and η_E are efficient. From Fig. 1, we can see the refined meshes appear around the origin and along the line $y = -1$, which are near the locations of singularity.

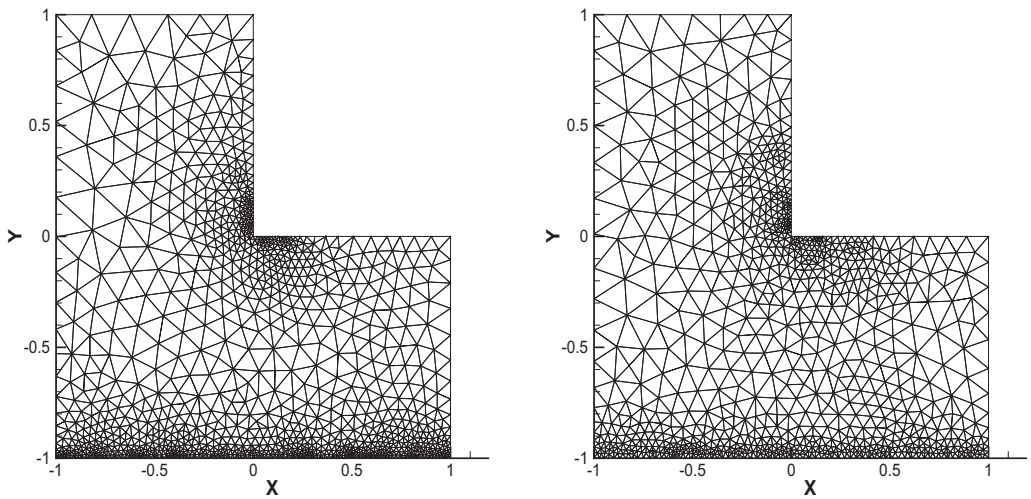

Fig. 1. Refinements via projection stabilized method with η_R(left) and η_E(right).

Table 3
Results for uniform refinements via projection stabilized method.

Level	DOF^j	$\boldsymbol{e}_r^j$	Order	$\eta_{R,r}$	E_R	$\eta_{E,r}$	E_E
0	166	0.4871	–	0.2972	0.6102	1.0193	1.4901
1	652	0.3108	0.6570	0.2158	0.6946	0.8059	1.8461
2	1526	0.2281	0.7272	0.1661	0.7284	0.6091	1.9001
3	2688	0.1719	0.9982	0.1321	0.7684	0.4912	2.0301
4	4258	0.1359	1.0217	0.1097	0.8069	0.4193	2.1907

Table 4
Results for adaptive refinements via projection stabilized method with η_R.

Level	DOF^j	$\boldsymbol{e}_r^j$	Order	$\eta_{R,r}$	E_R
0	176	0.4479	–	0.2955	0.6598
1	427	0.2315	1.4891	0.1763	0.7614
2	820	0.1365	1.6176	0.1248	0.9140
3	1322	0.1072	1.0112	0.1006	0.9384
4	2172	0.0804	1.1580	0.0781	0.9712

Table 5
Results for adaptive refinements via projection stabilized method with η_E.

Level	DOF^j	$\boldsymbol{e}_r^j$	Order	$\eta_{E,r}$	E_E
0	166	0.4871	–	0.7259	1.4901
1	317	0.3158	1.3394	0.5163	1.6346
2	592	0.1942	1.5563	0.3734	1.9222
3	974	0.1343	1.4812	0.3043	2.2651
4	1532	0.1080	0.9634	0.2482	2.2981

- The recovery-based error estimator η_R is more exact than the residual error estimator η_E. From Table 4, the effectivity index of η_R approaches 1.0 as the number of elements for triangulations increases. However, the effectivity index of η_E in Table 5 does not approach 1.0. Hence, η_R is asymptotically exact for the problem, while η_E is not.

Secondly, we use the adaptive strategy for the penalizing jump stabilized method. The left part of Fig. 2 shows the final adaptive mesh based on the estimator η_R. The refinements occur around the origin and along the line $y = -1$. Meanwhile, the right part of Fig. 2 compares the value of estimator η_R with the true error. It shows the estimated error based on η_R is close to the true error. This illustrates η_R also works well for the penalizing jump stabilized method.

4.4. A singular problem

In the third example, we consider Ω be a disk of radius 1 with a crack joining the center to the boundary as presented in [24] and the exact solution $\boldsymbol{u} = (u_1, u_2)$ and p are given as follows:

$$u_1 = 1.5r^{1/2}(\cos(0.5\theta) - \cos(1.5\theta)),$$
$$u_2 = 1.5r^{1/2}(3\sin(0.5\theta) - \sin(1.5\theta)),$$
$$p = -6r^{-1/2}\cos(0.5\theta),$$

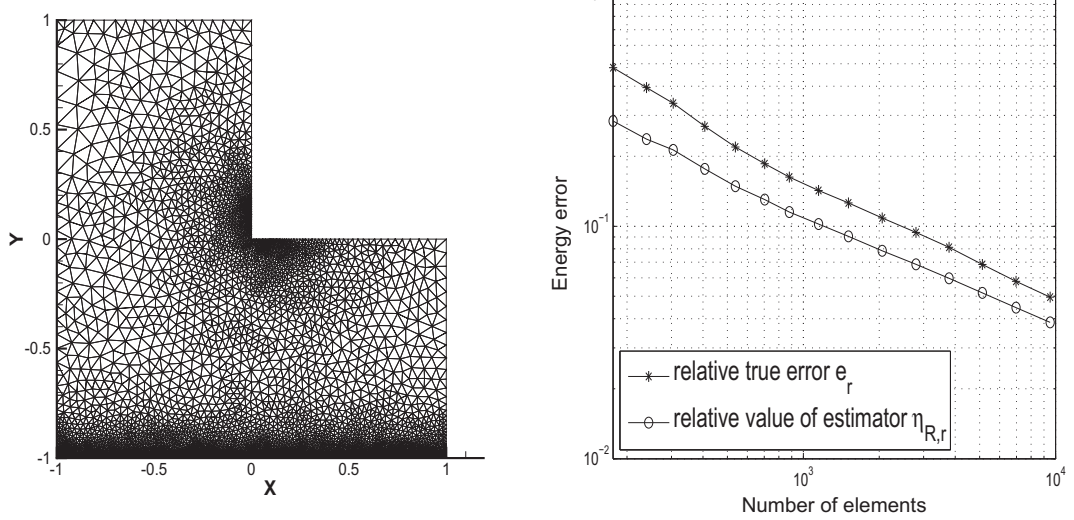

Fig. 2. Results by penalizing jump stabilized method with recovery-based estimator η_R.

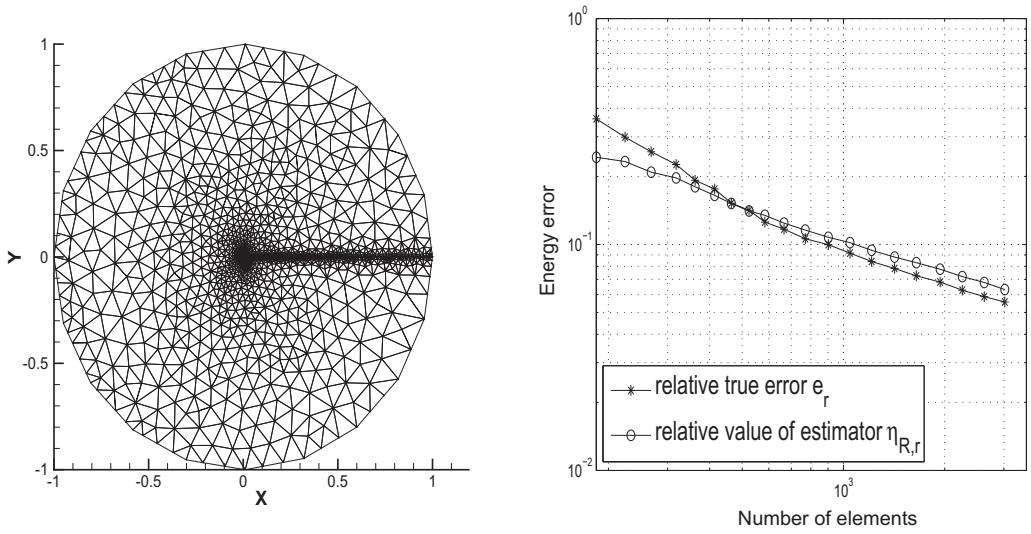

Fig. 3. Results by projection stabilized method with recovery-based estimator η_R.

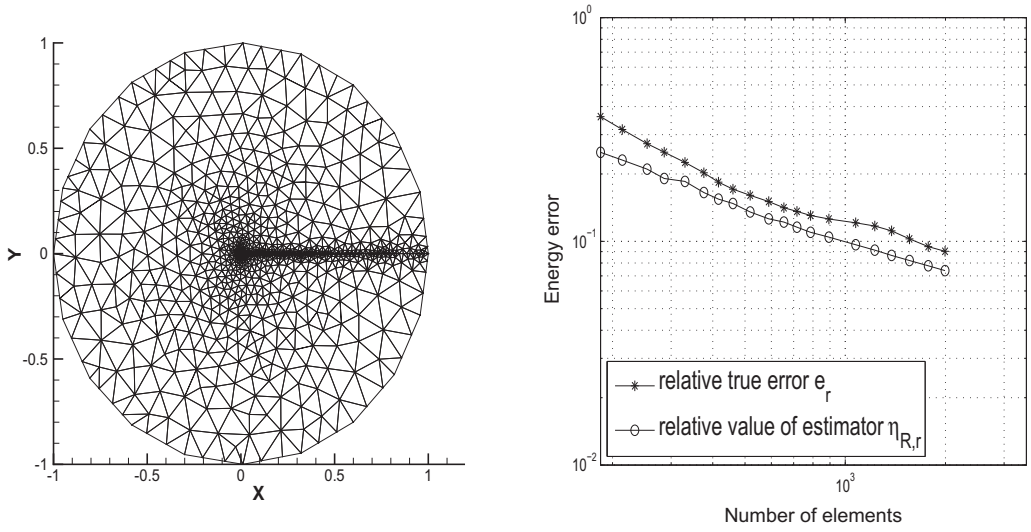

Fig. 4. Results by penalizing jump stabilized method with recovery-based estimator η_R.

where (r, θ) is a polar representation of a point in the disk. Obviously, the pressure is singular at the end of the crack; i.e., at the center of the disk (0,0). $\boldsymbol{f}$ is determined by (1) and $\boldsymbol{u}$ is enforced with appropriate inhomogeneous boundary conditions.

Fig. 3 and Fig. 4 show the results for adaptive refinements with η_R based on projection stabilized and penalizing jump stabilized method, respectively. From the left parts of both figures, we note that the local refinements appear near the crack due to the singularity of this problem. The right parts of both figures show the comparison of the value of estimator η_R and the true error. We can see that η_R is still asymptotically exact for the singular problem, independent of the choice of stabilization term.

To compare the effectivity index of η_R with that of the residual estimator η_E, we present the numerical results of the projection stabilized method with the η_E based adaptive strategy in Fig. 5. Comparing the right part of Fig. 5 with that of Fig. 3, we found that the recovery-based error estimator η_R is more exact than the residual error estimator η_E.

5. Conclusions

In this paper, we propose a recovery-based error estimator for the stabilized P_1/P_0 finite element approximations to the Stokes equation. It establishes the reliability and effectivity bounds of the estimator for both the penalizing jump and the projection stabilized methods. Moreover, it shows numerically that the recovery-based estimator η_R is more accurate than the residual estimator η_E. One advantage of the recovery-based error estimator is that no information of the underlying prob-

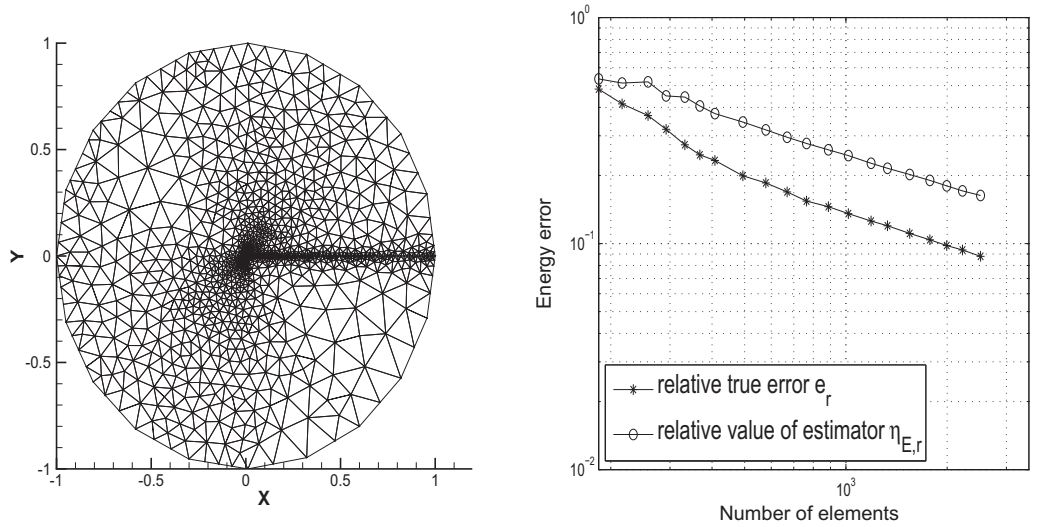

Fig. 5. Results by projection stabilized method with residual estimator η_E.

lem is needed. Therefore, it is easy to apply to other complex models such as Navier–Stokes problem, conduction convection problem.

When the underlying problem, e.g., the Stokes interface problem, is not smooth, the recovery-based estimator studied in this paper is no longer efficient. This is because the estimator will lead to over-refinements at where there are no errors. (For detailed discussion on the elliptic interface problem, see [7–9].) Therefore, for the Stokes interface problem, we need to recover a stress tensor, $G(\boldsymbol{\sigma}_h)$, in the conforming finite element spaces of $H(\mathrm{div};\Omega)^d$, instead of $C^0(\Omega)^{d\times d}$, and to use the proper norm. This modified recovery-based estimator will be studied in a forthcoming article.

References

[1] M. Ainsworth, J. Oden, A posteriori error estimation in finite element analysis, Wiley-Interscience, John Wiley & Sons, New York, 2000.
[2] C. Baiocchi, F. Brezzi, Stabilization of unstable numerical methods, in: P.E. Ricci (Ed.), Problemi Attuali dell'Analisi e dia Fisica Matematica, Universita La Sapienza, Roma, 1993, pp. 59–64.
[3] T. Barth, P. Bochev, M. Gunzburger, J. Shadid, A taxonomy of consistently stabilized finite element methods for the Stokes problem, SIAM J. Sci. Comput. 25 (2004) 1585–1607.
[4] C. Bernardi, R. Verfürth, Adaptive finite element methods for elliptic equations with non-smooth coefficients, Numer. Math. 85 (2000) 579–608.
[5] P. Bochev, M. Gunzburger, An absolutely stable pressure-poisson stabilized finite element method for the Stokes equations, SIAM J. Numer. Anal. 42 (2004) 1189–1207.
[6] P. Bochev, C. Dohrmann, M. Gunzburger, Stabilization of low-order mixed finite elements for the Stokes equations, SIAM J. Numer. Anal. 44 (2006) 82–101.
[7] Z. Cai, S. Zhang, Recovery-based error estimator for interface problems: conforming linear elements, SIAM J. Numer. Anal. 47 (2009) 2132–2156.
[8] Z. Cai, S. Zhang, Recovery-based error estimator for interface problems: mixed and nonconforming finite elements, SIAM J. Numer. Anal. 48 (2010) 30–52.
[9] Z. Cai, S. Zhang, Flux recovery and a posteriori error estimators: conforming elements for scalar elliptic equations, SIAM J. Numer. Anal. 48 (2010) 578–602.
[10] C. Carstensen, S. Funken, A posteriori error control in low-order finite element discretisations of incompressible stationary flow problems, Math. Comput. 70 (2000) 1353–1381.
[11] C. Carstensen, Some remarks on the history and future of averaging techniques in a posteriori finite element error analysis, Z. Angew. Math. Mech. 84 (2004) 3–21.
[12] C. Carstensen, R. Verfürth, Edge residuals dominate a posteriori error estimates for low order finite element methods, SIAM J. Numer. Anal. 36 (1999) 1571–1587.
[13] J. Douglas, J. Wang, An absolutely stabilized finite element method for the Stokes problem, Math. Comput. 52 (1989) 495–508.
[14] V. Girault, P.A. Raviart, Finite Element Methods for Navier–Stokes Equations, Springer-Verlag, Berlin, NewYork, 1986.
[15] F. Hecht, O. Pironneau, K. Ohtsuka, Freefem++, 2010. <http://www.freefem.org/ff++/ftp/>.
[16] T. Hughes, L. Franca, A new finite element formulation for CFD: VII. The Stokes problem with various well-posed boundary conditions: symmetric formulations that converge for all velocity/pressure spaces, Comput. Methods Appl. Mech. Eng. 65 (1987) 85–96.
[17] D. Kay, D. Silvester, A posteriori error estimation for stabilized mixed approximations of the Stokes equations, SIAM J. Sci. Comput. 21 (1999) 1321–1336.
[18] N. Kechkar, D. Silvester, Analysis of locally stabilized mixed finite element methods for the Stokes equations, Math. Comput. 58 (1992) 1–10.
[19] J. Li, Y. He, A stabilized finite element method based on two local Gauss integrations for the Stokes equations, J. Comput. Appl. Math. 214 (2008) 58–65.
[20] A. Naga, Z. Zhang, A posteriori error estimates based on polynomial preserving recovery, SIAM J. Numer. Anal. 9 (2004) 1780–1800.
[21] R. Rodríguez, Some remarks on Zienkiewicz–Zhu estimator, Numer. Methods PDEs Equ. 10 (1994) 625–635.
[22] L. Song, Y. Hou, H. Zheng, The two-grid stabilization of equal-order finite elements for the Stokes equations, Int. J. Numer. Methods Fluids 67 (2011) 2054–2061.
[23] R. Verfürth, A Review of A Posteriori Error Estimation and Adaptive mesh-Refinement Techniques, Wiley Teubner, 1996.
[24] R. Verürth, A posteriori error estimates for the Stokes equations, Numer. Math. 55 (1989) 309–325.

[25] J. Wang, Y. Wang, X. Ye, A posterior error estimate for stabilized finite element methods for the Stokes equations, Int. J. Numer. Anal. Model. 9 (2012) 1–16.
[26] H. Zheng, L. Shan, Y. Hou, A quadratic equal-order stabilized method for Stokes problem based on two local Gauss integrations, Numer. Methods PDEs Equ. 26 (2010) 1180–1190.
[27] H. Zheng, Y. Hou, F. Shi, A posteriori error estimates of low-order mixed finite elements for incompressible flow, SIAM J. Sci. Comput. 32 (2010) 1346–1360.
[28] O. Zienkiewicz, J. Zhu, The superconvergence patch recovery and a posteriori error estimates, Part I: the recovery technique, Int. J. Numer. Methods Eng. 33 (1992) 1331–1364.
[29] O. Zienkiewicz, J. Zhu, The superconvergence patch recovery and a posteriori error estimates, Part II: error estimates and adaptivity, Int. J. Numer. Methods Eng. 33 (1992) 1365–1382.